IEEE Photonics Journal
An IEEE Photonics Society Publication

Open Access

Label-Free Si_3N_4 Photonic Crystal Based Immunosensors for Diagnostic Applications

Volume 6, Number 6, December 2014

D. Zecca
A. Qualtieri
G. Magno
M. Grande
V. Petruzzelli
B. Prieto-Simon
A. D'Orazio
M. De Vittorio
N. H. Voelcker
T. Stomeo

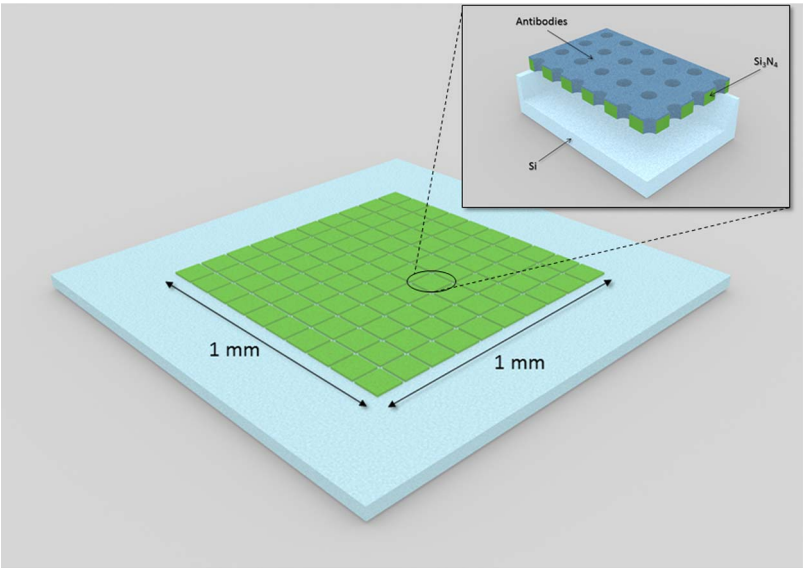

DOI: 10.1109/JPHOT.2014.2352625
1943-0655 © 2014 IEEE

IEEE photonics SOCIETY

IEEE

Label-Free Si_3N_4 Photonic Crystal Based Immunosensors for Diagnostic Applications

D. Zecca,[1,2] A. Qualtieri,[1] G. Magno,[3] M. Grande,[3] V. Petruzzelli,[3] B. Prieto-Simon,[4] A. D'Orazio,[3] M. De Vittorio,[1,5,6] N. H. Voelcker,[4] and T. Stomeo[1]

[1]Center for Bio-Molecular Nanotechnology, Istituto Italiano di Tecnologia (IIT), 73010 Arnesano (Lecce), Italy
[2]Politecnico di Torino, Scuola di Dottorato, 10129 Torino, Italy
[3]Dipartimento di Ingegneria Elettrica e dell'Informazione, Politecnico di Bari, 70125 Bari, Italy
[4]Mawson Institute, University of South Australia, Adelaide, SA 5001, Australia
[5]Dipartimento di Ingegneria dell'Innovazione, Università del Salento, 73100 Lecce, Italy
[6]National Nanotechnology Laboratory, Istituto Nanoscienze-CNR, 73100 Lecce, Italy

DOI: 10.1109/JPHOT.2014.2352625

Manuscript received June 10, 2014; revised August 8, 2014; accepted August 8, 2014. Date of publication September 5, 2014; date of current version December 18, 2014. This work was supported by the Regione Puglia-South Australia Research Collaboration Award titled "Photonic Crystal Biosensors for Cardiac Biomarker Detection," a cooperation among Istituto Italiano di Tecnologia-CBN, Mawson Institute-University of South Australia, and Politecnico di Bari, and by the ITEM project "Infrastructure for BioMEMS technologies of advanced sensing for environmental and food monitoring and diagnostic (PONa3_00077)." Corresponding author: D. Zecca (e-mail: davide.zecca@iit.it).

Abstract: Immunosensors are devices that exploit immobilized antibodies to promote the binding of specific analytes related to diseases of medical importance, such as cancer or cardiac dysfunctions. Label-free immunosensors have an important role, due to their simplicity and fast read-out. Here, the proof of concept for an immunosensor based on a 2-D photonic crystal silicon nitride membrane is presented. The device has been fabricated by means of a well-tuned nanofabrication protocol, achieving a high-quality photonic pattern on a large-area membrane (1 mm $\times$ 1 mm), and it has been tested for the detection of interleukin-6, getting protein detection at pg/mL concentrations.

Index Terms: Photonic crystals (PhC), biosensors, fabrication and characterization.

1. Introduction

The monitoring of biomarkers is becoming the key point to prevent, diagnose and monitor important pathologic states, providing bio-chemical assays faster and cheaper than conventional laboratory tests and opening a new trend of innovative point-of-care platforms called immunosensors [1]. These biosensors use antibodies as bioreceptors [2] to provide selectivity and high affinity to the biorecognition event. The remarkable binding properties of antibodies and the possibility to produce them for a wide range of analytes have promoted the design of immunosensors for diverse types of assays and the application in monitoring areas such as health [3], [4], environment [5] and food [6], [7] analysis. Immunosensors can be subdivided according to the model of transduction such as piezoelectric, electrochemical or optical sensors. In this last class, label-free optical biosensors are particularly attractive since they use a method based on

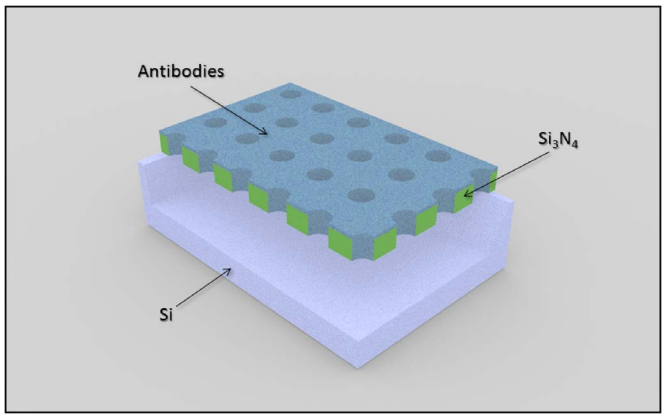

Fig. 1. Sketch of the membrane structure functionalized with antibodies against IL-6.

the variation of their optical properties that scales with analyte concentration [8]. A number of different label-free optical sensors have been proposed and developed, with approaches based on surface plasmon resonance [9], ring resonators [10], slot waveguides [11], interferometric sensors exploiting porous silicon or porous alumina [12], [13], and ultra-high-Q whispering-gallery-mode resonators [14].

In the last years photonic crystal (PhC)-based label-free biosensors have been also investigated in different configurations, such as cavity [15]–[18], line-defect [19] and slab [20].

Photonic crystals [21], [22] are structures composed by a periodic arrangement of materials with different refractive indexes (n) and able to transmit or reflect well determined electromagnetic wavelength ranges by tuning their geometrical parameters such as the periodicity p or the radius r. These properties make them good candidates for designing photonic immunosensors with a strong coupling between guided and radiated modes that are very sensitive to environment variations.

In this work, the design, fabrication and testing of a label-free membrane immunosensor, able to detect proteins in solution, is described. A sketch of the realized biosensor is shown in Fig. 1. It is based on a two dimensional (2D) PhC in membrane configuration [23]–[25] patterned on a large area of 1 mm^2 on a silicon (Si) substrate. The structure has been made in silicon nitride (Si_3N_4), which is a suitable material for this application thanks to its biocompatibility, high refractive index $(n \sim 2)$ and mechanical properties.

The sensor surface and the hole sidewalls have been functionalized to covalently bind antibodies that allow the selective recognition of the analyte in a phosphate buffer saline (PBS) solution. In this case, the biomarker used during the experimental tests is the interleukin-6 (IL-6) protein, which is a cytokine produced by cells in some pathologies such as oral cancer and Alzheimer, as further detailed in Section 3.

The detection of the IL-6 was performed in reflection mode, evaluating the wavelength shift of the resonance peaks (Fano resonances), in visible (VIS) and near-infrared (NIR) spectra, caused by exposure of the anti-IL-6 antibody functionalized sensor to different concentrations of IL-6 protein.

The choice to use a membrane slab instead of a microcavity structure was led from the need to collect signal from the entire large surface using a simple and cost-effective read-out system. In fact, in the microcavity case, the signal mainly comes from the analyte bound in the cavity area where the electromagnetic field is localized. Moreover, the optics to collimate and align a little light spot with the cavity is necessary, increasing the cost and affecting the portability of the system.

Even if enzyme-linked immunosorbent assay (ELISA) [26] is already used to detect IL-6 in clinical assays, this is not a real-time method, usually involving time-consuming protocols. For these reasons, a label-free approach able to detect IL-6 in real-time at very low concentrations (e.g., IL-6 concentration in serum of a healthy individual is < 6 pg/mL, while in patients with oral cancer it ranges from 20 to over 1000 pg/mL) [27] would be a powerful tool for clinical diagnosis.

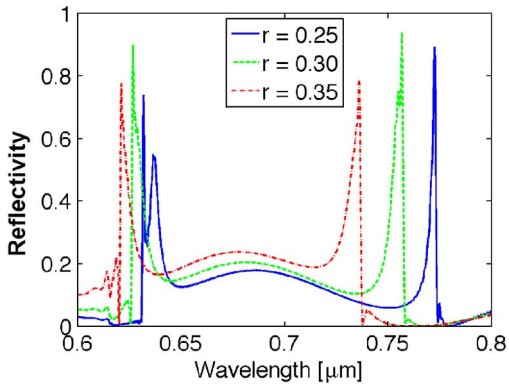

Fig. 2. Simulated reflectance spectra of the PhC in PBS solution for different radii (red dash-dot line for $r = 0.35^{*}p$, green dashed line for $r = 0.30^{*}p$, and blue solid line for $r = 0.25^{*}p$) and $p = 460$ nm.

2. Numerical Simulations and Nano-Fabrication Protocol

A numerical analysis based on the Finite Difference Time Domain (FDTD) method has been used to investigate the behavior of the sensor in the VIS-NIR spectral range: the simulations have been performed in a PBS environment (refractive index $n \sim 1.34$) by changing the radius r of the holes and the periodicity p, aiming to obtain sharp Fano resonances in the wavelength range of interest. During simulations, the thickness of the Si_3N_4 membrane has been set to 300 nm, satisfying both optical and mechanical requests. In fact, a thin membrane increases the sensitivity and quality factor, but it could suffer of bowing in the periodicity plane, causing a degradation of the performance and even the formation of cracks, especially when large suspended areas are required.

The described analysis allowed to design a structure that shows resonant wavelengths located at about 640 nm (the 1st peak) and 760 nm (the 2nd peak) for a $p = 460$ nm and r equal to $0.35^{*}p$, $0.30^{*}p$, and $0.25^{*}p$ as shown in Fig. 2.

Once the geometrical parameters were defined, the 2D PhC immunosensor was fabricated using an optimized process protocol, which allowed us to achieve a high quality photonic structure on a large Si_3N_4 membrane area (1 mm $\times$ 1 mm).

We started the fabrication process by writing the 2D PhC pattern by means of electron beam lithography (EBL) exposure on a 400 nm-thick ZEP520A resist layer. Then the pattern was transferred into the Si_3N_4 layer via anisotropic inductively coupled plasma (ICP) etching. Finally, the chip was immersed in a tetramethylammonium hydroxide (TMAH) solution that, by means of a wet etching, removed the underlying layer of Si by allowing the membrane release.

During the optimization process, we have experimentally verified that there is not a cavity effect between the patterned silicon slab and the etched silicon substrate. In fact, the developed wet etching process makes the etched silicon surface very rough leading to an experimental reflectance lower than 5% over the whole spectral range of interest. This reflectance has been measured after removing the patterned Si_3N_4 slab. Fig. 3 shows an in-plane image of the fabricated 2D PhC membrane acquired by means of scanning electron microscopy (SEM): the inset shows the SEM cross-section image of the membrane obtained by means of focussed ion beam (FIB) milling.

In Fig. 4 is reported a sketch of the realized immunosensor large membrane consisting of a 10 $\times$ 10 matrix where each green square represents a 100 μm $\times$ 100 μm PhC membrane. This approach gives us the chance to get a large sensing area without structural problems and with good optical properties.

3. Experimental Results

Structures with period $p = 460$ nm and $r = 0.25^{*}p$ have been fabricated and tested. The measurements have been performed at normal incidence focusing a tungsten white lamp spot

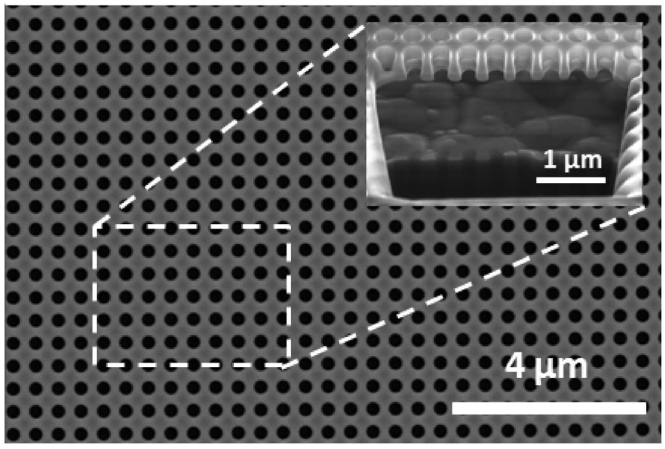

Fig. 3. SEM in-plane image of the fabricated 2D PhC membrane: the inset shows the SEM cross-section image of the membrane acquired by means of focussed ion beam milling.

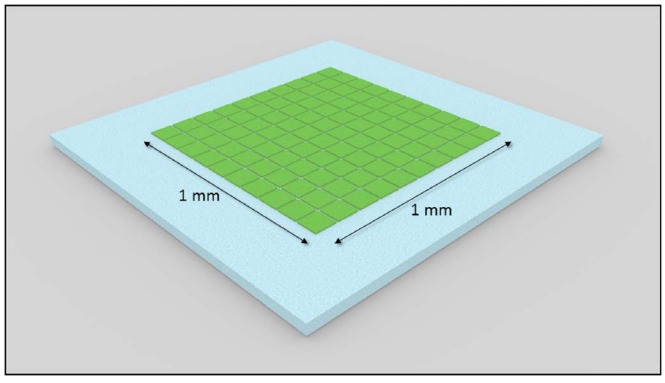

Fig. 4. Sketch of the 10 $\times$ 10 PhC matrix where each green square represents a 100 μm $\times$ 100 μm PhC membrane.

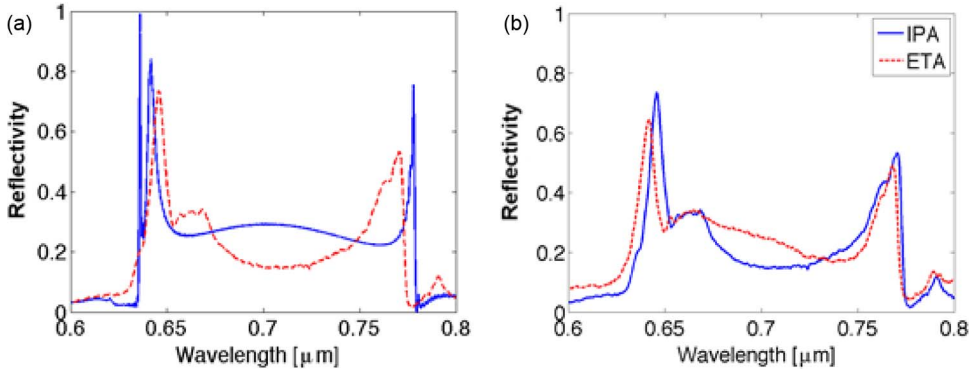

Fig. 5. (a) Theoretical (blue solid line) and experimental (red dashed line) reflection spectra of the 2D PhC biosensor with $p = 460$ nm and $r = 0.25 * p$ when the sensor is immersed in IPA solution. (b) Experimental spectra when the sensor is immersed in IPA (blue solid line) and ethanol (red dashed line) revealing wavelength shift.

(filtered from 400 nm to 750 nm) on the chip. Then, the reflected light has been collected by an aspherical fiber lens and sent to an optical spectrometer via an optical multimode fiber. In Fig. 5(a) is reported a typical reflection spectrum at normal incidence acquired when the

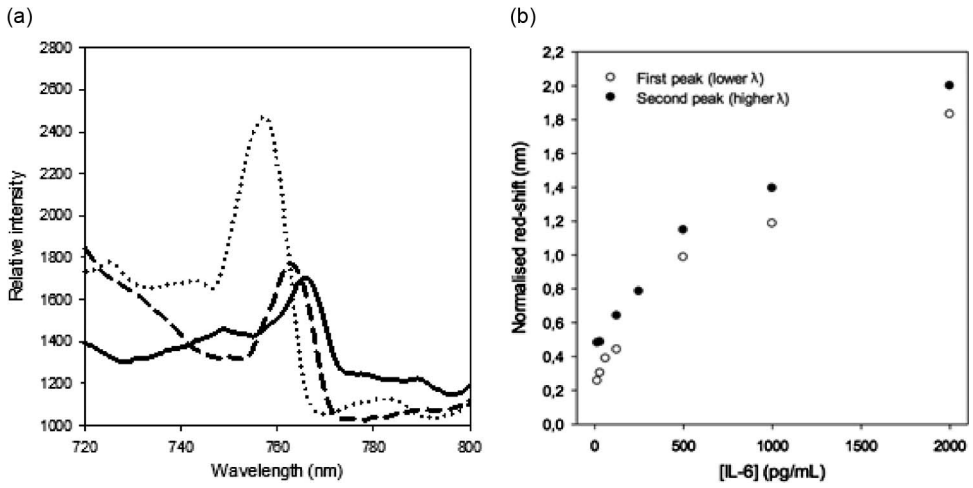

Fig. 6. (a) Measurement in PBS solution about the evolution of the second resonant peak along the PhC functionalization: prior to plasma polymerization (dotted line), after plasma polymerization (dashed line) and after antibody immobilization (solid line). (b) Calibration curve of normalized red-shift versus IL-6 in buffer solution based on the evolution of the two resonant peaks characteristic of the developed PhC immunosensor.

sensor was immersed in isopropanol (IPA) solution. The experimental spectrum (red line) shows Fano resonances in the visible spectrum at about 640 nm for the 1st peak and around 760 nm for the 2nd peak in good agreement with the simulation (blue line), while the small discrepancy between the experiment and simulations is due to the fabrication tolerances and to the intrinsic losses (k, extinction coefficient) of the Si_3N_4 slab. The sensor has also been tested in IPA and ethanol, revealing a wavelength shift as the refractive index is varied as reported in Fig. 5(b). These results also demonstrate the ability of the device to sense the variation of the refractive index of the solution in which the sensor is immersed.

The fabricated 2D PhC was functionalized by plasma polymerization, using allyl glycidyl ether as the monomer. Initially, the deposition was optimized to reduce the thickness of the polymer while providing a high density of available epoxide groups. Control of the deposition time allowed polymer thicknesses below 100 nm. A thickness of 60 nm was considered adequate to allow penetration into the cavities, while avoiding their blockage. Moreover, we also checked the position of the resonant peaks after polymerization at different spots, finding a relative standard deviation (RSD) similar to that found prior to polymerization (RSD $= 0.1\%$ obtained over 10 measurements), thus confirming the homogeneity of the polymer around the PhC. As shown in Fig. 6(a), the resonant peak is shifted towards higher wavelength values, confirming the modification, while keeping the photonic crystal features. The presence of the polymer on the surface resulted in an increase in the dielectric permittivity that caused a red-shift of the reflected peak wavelength values. Epoxide groups reacted with primary amine groups from the antibody at a moderate alkaline pH (100 μg/mL antibody solution in 0.05 M carbonate buffer, pH 9.6). Remaining epoxide groups were blocked by 30 minutes incubation in 1 M ethanolamine solution.

The red-shift of both resonant peaks was followed after consecutive IL-6 incubations, providing the calibration curve shown in Fig. 6(b). The sensitivity of the assay, calculated as the initial slope of the plots in Fig. 6(b), is $2.1 \cdot 10^{-3}$ nm/(pg/mL). The detection limit determined as 3σ/sensitivity is equal to 1.5 pg/mL, where σ is the standard deviation for the blank (PBS solution without IL-6). Results are similar to those obtained for other biosensors using a PhC slab and a reflectance-based read-out configuration [28]. Moreover, as in a ill patient the concentration of IL-6 is higher than 1 pg/mL, it is possible to assume that our device can properly work as biosensor, proving to be the proof-of-concept for a medical aid device.

4. Conclusion

In conclusion, we have reported on the design, fabrication and characterization of an immunosensor for the fast and accurate detection of biomarkers related to the diagnosis and prevention of complex diseases, such as cancer and Alzheimer. To this purpose, a powerful sensing platform characterized by a large (1 mm^2) Si_3N_4 2D-PhC membrane working in the VIS-NIR spectral range, has been fabricated by means of a high standard fabrication protocol. The experimental results are in good agreement with the numerical simulations, highlighting the versatility of the photonic immunosensor to sense the variation of the refractive index of the solution in which it is immersed. The large 2D-PhC membrane has also been functionalized by plasma polymerization and coated with anti-IL-6 antibodies for the detection of IL-6 protein in solution, demonstrating good sensitivity and reproducibility. We believe that the proposed label-free immunosensor may offer a very promising way for the realization of innovative devices able to reduce cost and time in medical diagnosis.

References

[1] P. B. Luppa, L. J. Sokoll, and D. W. Chan, "Immunosensors—Principles and applications to clinical chemistry," *Clinica Chimica Acta*, vol. 314, no. 1–2, pp. 1–26, Dec. 2001.

[2] P. J. Conroy, S. Hearty, P. Leonard, and R. J. O'Kennedy, "Antibody production, design and use for biosensor-based applications," *Seminars Cell Developmental Biol.*, vol. 20, no. 1, pp. 10–26, Feb. 2009.

[3] J. Wang, "Amperometric biosensors for clinical and therapeutic drug monitoring: A review," *J. Pharmaceutical Biomed. Anal.*, vol. 19, no. 1–2, pp. 47–53, Feb. 1999.

[4] C. Parsajoo and J.-M. Kauffmann, "Biosensors for drug testing and discovery," *Biosensors Med. Appl., Vol. Woodhead Publishing Series in Biomaterials*, pp. 233–262, 2012.

[5] S. Rodriguez-Mozaz, M.-P. Marco, M. J. L. de Alda, and D. Barceló, "Biosensors for environmental monitoring of endocrine disruptors: A review article," *Analytical Bioanalytical Chemistry*, vol. 378, no. 3, pp. 588–598, Feb. 2004.

[6] S. S. Moises and M. Schäferling, "Toxin immunosensors and sensor arrays for food quality control," *Bioanalytical Rev.*, vol. 1, no. 1, pp. 73–104, Dec. 2009.

[7] L. D. Mello and L. T. Kubota, "Review of the use of biosensors as analytical tools in the food and drink industries," *Food Chemistry*, vol. 77, no. 2, pp. 237–256, May 2002.

[8] X. Fan *et al.*, "Sensitive optical biosensors for unlabeled targets: A review," *Analytica Chimica Acta*, vol. 620, no. 1–2, pp. 8–26, Jul. 2008.

[9] J. Homola, S. S. Yee, and G. Gauglitz, "Surface plasmon resonance sensors: Review," *Sens. Actuators B, Chemical*, vol. 54, no. 1–2, pp. 3–15, Jan. 1999.

[10] H. J. Lee *et al.*, "A planar split-ring resonator-based microwave biosensor for label-free detection of biomolecules," *Sens. Actuators B, Chemical*, vol. 169, pp. 26–31, Jul. 2012.

[11] A. L. Washburn and R. C. Bailey, "Photonics-on-a-chip: Recent advances in integrated waveguides as enabling detection elements for real-world, lab-on-a-chip biosensing applications," *Analyst*, vol. 136, no. 2, pp. 227–236, Jan. 2011.

[12] A. Jane, R. Dronov, A. Hodges, and N. H. Voelcker, "Porous silicon biosensors on the advance," *Trends Biotechnol.*, vol. 27, no. 4, pp. 230–239, Apr. 2009.

[13] R. Dronov, J. G. Shapter, A. Hodges, and N. H. Voelcker, "Nanoporous alumina-based interferometric transducers ennobled," *Nanoscale*, vol. 3, no. 8, pp. 3109–3114, Aug. 2011.

[14] A. Schweinsberg *et al.*, "An environmental sensor based on an integrated optical whispering gallery mode disk resonator," *Sens. Actuators B, Chemical*, vol. 123, no. 2, pp. 727–732, May 2007.

[15] L. Martiradonna *et al.*, "Spectral tagging by integrated photonic crystal resonators for highly sensitive and parallel detection in biochips," *Appl. Phys. Lett.*, vol. 96, no. 11, pp. 113 702–113 704, Mar. 2010.

[16] M. Lee and P. M. Fauchet, "Two-dimensional silicon photonic crystal based biosensing platform for protein detection," *Opt. Exp.*, vol. 15, no. 8, pp. 4530–4535, Apr. 2007.

[17] D. Dorfnera *et al.*, "Photonic crystal nanostructures for optical biosensing applications," *Biosens. Bioelectron.*, vol. 24, no. 12, pp. 3688–3692, Aug. 2009.

[18] F. Pisanello, M. De Vittorio, and R. Cingolani, "Modal selective tuning in a photonic crystal cavity," *Superlattices Microstruct.*, vol. 47, no. 1, pp. 34–38, Jan. 2010.

[19] N. Skivesen *et al.*, "Photonic-crystal waveguide biosensor," *Opt. Exp.*, vol. 15, no. 6, pp. 3169–3176, Mar. 2007.

[20] M. E. Beheiry, V. Liu, S. Fan, and O. Levi, "Sensitivity enhancement in photonic crystal slab biosensors," *Opt. Exp.*, vol. 18, no. 22, pp. 22 702–22 714, Oct. 2010.

[21] E. Yablonovitch, "Inhibited spontaneous emissions in solid-state physics and electronics," *Phys. Rev. Lett.*, vol. 58, no. 20, pp. 2059–2062, May 1987.

[22] J. D. Joannopoulos, S. G. Johnson, J. N. Winn, and R. D. Meade, *Photonic Crystals: Molding the Flow of Light (Second Edition)*. Princeton, NJ, USA: Princeton Univ. Press, 2008.

[23] T. Stomeo *et al.*, "Novel optical filter based on two coupled PhC GaAs-membranes," *Opt. Lett.*, vol. 35, no. 3, pp. 411–413, Feb. 2010.

[24] A. Qualtieri *et al.*, "Emission control of colloidal nanocrystals embedded in Si_3N_4 photonic crystal H1 nanocavities," *Microelectron. Eng.*, vol. 87, no. 5–8, pp. 1435–1438, May–Aug. 2010.

[25] F. Pisanello *et al.*, "Silicon nitride PhC nanocavities as versatile platform for visible spectral range devices," *Photon. Nanostruct. Fundamentals Appl.*, vol. 10, no. 3, pp. 319–324, Jun. 2012.
[26] A. Voller, A. Bartlett, and D. E. Bidwell, "Enzyme immunoassays with special reference to ELISA techniques," *J. Clinical Pathology*, vol. 31, no. 6, pp. 507–520, Jun. 1978.
[27] F. Riedel *et al.*, "Serum levels of interleukin-6 in patients with primary head and neck squamous cell carcinoma," *Anticancer Res.*, vol. 25, no. 4, pp. 2761–2765, Jul.–Aug. 2005.
[28] B. Cunningham, P. Li, B. Lin, and J. Pepper, "Colorimetric resonant reflection as a direct biochemical assay technique," *Sens. Actuators B, Chemical*, vol. 81, no. 2–3, pp. 316–328, Jan. 2002.